Available online at www.sciencedirect.com
ScienceDirect
Proceedings of the Combustion Institute 31 (2007) 1215–1222
Proceedings of the Combustion Institute
www.elsevier.com/locate/proci

High temperature ignition and combustion enhancement by dimethyl ether addition to methane–air mixtures ☆

Zheng Chen, Xiao Qin, Yiguang Ju *, Zhenwei Zhao, Marcos Chaos, Frederick L. Dryer

Department of Mechanical and Aerospace Engineering, Princeton University, Princeton, NJ 08544, USA

Abstract

The effects of dimethyl ether (DME) addition on the high temperature ignition and burning properties of methane–air mixtures were studied experimentally and numerically. The results showed that for a homogeneous system, a small amount of DME addition to methane resulted in a significant reduction in the high temperature ignition delay. The ignition enhancement effect by DME addition was found to exceed that possible with equivalent amounts of hydrogen addition, and it was investigated by using radical pool growth and computational singular perturbation analysis. For a non-premixed methane–air system, it was found that two different ignition enhancement regimes exist: a kinetic limited regime and a transport limited regime. In contrast to the dramatic ignition enhancement in the kinetic limited regime, the ignition enhancement in the transport limited regime was significantly less effective. Furthermore, laminar flame speeds as well as Markstein lengths were experimentally measured for methane–air flames with DME addition. The results showed that the flame speed increases almost linearly with DME addition. However, the Markstein length and the Lewis number of the binary fuel change dramatically at small DME concentrations. Moreover, comparison between experiments and numerical simulations showed that only the most recent DME mechanism well reproduced the flame speeds of both DME–air and CH_4–air flames.

Keywords: Dimethyl ether; Ignition enhancement; Laminar flame speed; Markstein length

1. Introduction

Environmental regulations and energy diversity produce an urgent need to develop new clean fuels. Dimethyl ether (DME), which has low soot emission, no air or ground-water pollution effects, and can be mass produced from natural gas, coal, or biomass [1–5], is emerging as a substitute for liquefied petroleum gas (LPG), diesel fuels, and liquid natural gas (LNG). In addition, DME can also be used as an ignition enhancer in propulsion systems and internal combustion engines [6]. Recently, the study of DME combustion has received significant attention [1–6]. In kinetic research, several detailed chemical mechanisms for low and high temperature DME oxidation [7–11] have been developed and validated against burner stabilized flames [12,13], non-premixed

☆ Supplementary data for this article can be accessed online. See Appendix A.

* Corresponding author. Fax: +1 609 258 6233.
E-mail address: yju@princeton.edu (Y. Ju).

1540-7489/$ - see front matter © 2006 The Combustion Institute. Published by Elsevier Inc. All rights reserved.
doi:10.1016/j.proci.2006.07.177

counterflow flame ignition [14], and laminar flame speeds [15–17]. More recently, DME jet diffusion flames were also studied [18]. It was shown that due to the existence of oxygen atoms in DME, lift-off characteristics are distinctly different from other hydrocarbon fuels.

DME has shown promise as an additive and/or fuel extender. Recently, Yao and Qin [19] have undertaken studies on DME addition to methane for homogeneous charge compression ignition (HCCI) engines. In such cases, the coupling of DME kinetics with those of methane involves the low temperature kinetics of DME. On the other hand, DME/methane utilization in burners and in gas turbine applications is expected to involve principally high temperature kinetic coupling effects. For example, the effects of DME on the high temperature ignition of methane have been experimentally studied by Amano and Dryer [6], who showed that DME was an effective promoter of high temperature methane ignition. However, the underlying kinetic coupling between DME and CH_4 responsible for the observed ignition enhancement was not explored in any detail. In addition, kinetic coupling effects on flame properties and auto-ignition in non-premixed systems have not been studied. Moreover, the existing kinetic mechanisms have not been validated against the flame speeds of DME/CH_4 mixtures.

It is well known that flame properties such as burning rate and flame stability depend on the overall activation energy and the Lewis number (*Le*) [20]. Kinetic coupling may result in a dramatic change in the overall activation energy with a small amount of DME addition to methane. DME has a molecular weight larger than air so that the *Le* is larger than unity for lean DME/air mixtures in comparison to methane/air mixtures. On the other hand, DME is expected to react more quickly in the preheating zone decomposing to form lighter molecules. Therefore, it is of interest to investigate how the effective mixture Lewis number depends on the DME content in binary fuels with disparate molecular weights, such as DME/CH_4 mixtures.

The objective of the present study was to investigate kinetic coupling effects of DME addition on the high temperature ignition and burning properties of methane–air mixtures. Experimentally measured laminar flame speeds of DME–air and CH_4–air mixtures were compared with predictions by existing DME mechanisms including a recently developed model by Zhao et al. [21]. The latter mechanism is then used to study the effect of DME addition on the ignition enhancement in both homogeneous and non-homogeneous systems. Finally, the flame speeds of DME/CH_4–air mixtures were measured by using outwardly propagating spherical flames. The results were compared with model predictions and the effect of kinetic coupling on the Markstein length and Lewis number was studied.

2. Experimental/computational methods and kinetic model selection

The laminar flame speed and Markstein length of DME/CH_4–air premixed flames were measured by using outwardly propagating spherical flames in a dual-chambered, pressure-release-type, and high pressure combustion facility [17]. Pre-mixtures were prepared by using the partial pressure method from pure methane and DME compressed gas sources. The purities of the DME and CH_4 were 99.8% and 99.9%, respectively. Experiments were conducted for DME/CH_4–air mixtures: $\{\alpha CH_3OCH_3 + (1-\alpha)CH_4\} + \text{air}$, with values of the volume fraction, α, ranging from zero to one. The combustible mixture was spark-ignited at the center of the chamber with the minimum ignition energy so as to preclude significant ignition disturbances. The flame propagation sequence was imaged by using Schlieren photography. A high-speed digital video camera operating at 8000 frames per second was used to record the propagating flame images. To avoid possible effects caused by the initial spark disturbance and wall interference, data reduction was performed only for flame radii between 1.5 and 2.5 cm. The pressure rise in the combustion chamber was monitored using a pressure sensor. At the small flame radii studied in this work, the pressure rise is about 2%, resulting in a nearly constant pressure flame propagation condition.

The stretched flame speed was first obtained from the flame history and then was linearly extrapolated to zero stretch rate to obtain the unstretched flame speed [17,22]. The results presented here are the averaged value of at least two tests at each experimental condition. The estimated experimental error for flame speed determinations is approximately 5%. All experiments were performed at an initial temperature of 298 ± 3 K and at atmospheric pressure. In order to examine the available kinetic mechanisms, the measured flame speeds were compared with the numerical results obtained using PREMIX [23]. The Markstein length and the effective Lewis number of the binary fuel mixtures were then extracted from the measured flame speed data.

The effect of adding DME on ignition enhancement of methane was investigated numerically in two different systems, a homogeneous flame configuration to examine the kinetic ignition enhancement, and a non-premixed counterflow configuration to examine the effect of transport. The ignition time of homogeneous mixtures at constant pressure and enthalpy was calculated by using SENKIN [24]. For the non-premixed simulations, the quasi-steady temperature and

species distributions of counterflowing DME/CH_4 (298 K at the boundary) and hot air jets (1400 K at the boundary) were determined under a frozen flow constraint. At time zero, chemical reactions were allowed in the pre-calculated frozen flow field. Ignition time was recorded when the first increase in the temperature field exceeded 400 K, indicating thermal runaway. Simulations were conducted using an unsteady potential counterflow flame code described by Ju et al. [25,26]. To further examine the effect of flow residence time on ignition enhancement, the stretch rate in the frozen flow configuration was varied from low stretch to that near the ignition limit.

In order to properly model and interpret the present work, the chemical kinetic model used in the calculations must be capable of predicting the pure fuel–air laminar flame speed and high temperature shock tube ignition properties. One might expect that comprehensively developed detailed mechanisms for DME oxidation would also be capable of predicting high temperature kinetic properties for methane oxidation. The measured laminar flame speeds of pure DME–air and CH_4–air mixtures at atmospheric pressure and room temperature are shown in Figs. 1 and 2, respectively, along with the predictions utilizing a number of different DME mechanisms.

It is seen that the earlier DME mechanisms published by Curran and co-workers [8–10,14] (2000-Mech and 2003-Mech) are not able to well reproduce measured flame speeds for both lean and rich mixtures. Although a more recently updated version (2005-Mech [11]) predicts flame speeds much better than the previous ones, there is still a large discrepancy for lean DME–air and CH_4–air flames. Recent theoretical studies of the unimolecular decomposition of DME using the RRKM/master equation approach [21,27] yield significantly different parameters from those used

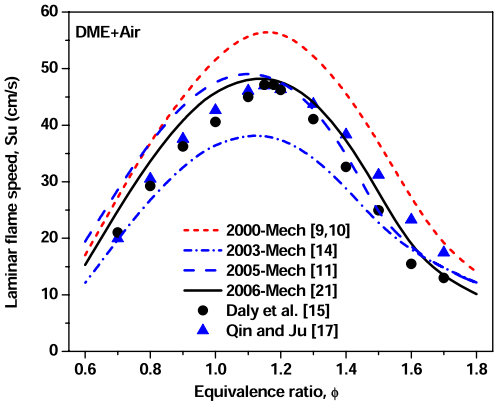

Fig. 1. Laminar flame speeds of DME–air mixtures as a function of equivalence ratio at 298 K, atmospheric pressure.

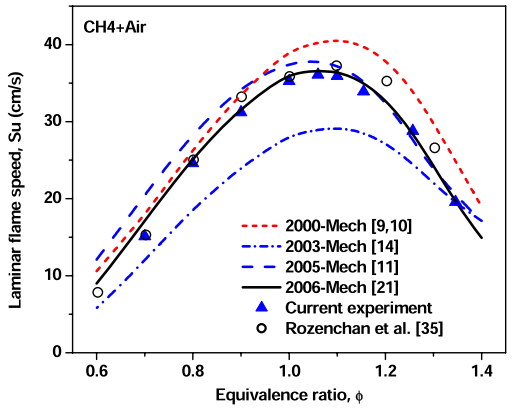

Fig. 2. Laminar flame speeds of CH_4–air mixtures as a function of equivalence ratio at 298 K, atmospheric pressure.

in the above models. Because decomposition and abstraction pathways are coupled during both pyrolysis and oxidation, considerable re-assessment, and updating of other parameters important to high-temperature oxidation are needed to incorporate this change. A new model that includes the revised decomposition parameters, updates in the sub-model and thermochemistry for the hydrogen oxidation [28], and a revised C_1–C_2 species sub-model developed in recent experimental and modeling studies on ethanol pyrolysis and oxidation [29–31], has been developed [21,27]. The mechanism was constructed and tested hierarchically against a large volume of experimental data for hydrogen, carbon monoxide, formaldehyde, and methanol oxidation. The new DME reaction mechanism (denoted here as 2006-Mech) consists of 290 reversible elementary reactions and 55 species, and its predictions compare well with high-temperature flow reactor data for DME pyrolysis and oxidation [9], for oxidation at high temperatures in a jet-stirred reactor [7], for high-temperature shock tube ignition [2,32], for species profiles from burner-stabilized flames [12,13], and for laminar flame speeds of DME-air flame (Fig. 1). The model also results in excellent prediction of CH_4–air flame speed data (Fig. 2). On the basis of the ability to reproduce these same reference conditions, we utilize the 2006-Mech in the remainder of comparisons reported in this paper.

3. Results and discussion

3.1. Ignition enhancement by DME addition

Figure 3 shows the effects of DME addition on the ignition time of homogeneous and non-homogeneous DME/CH_4–air mixtures. The results of

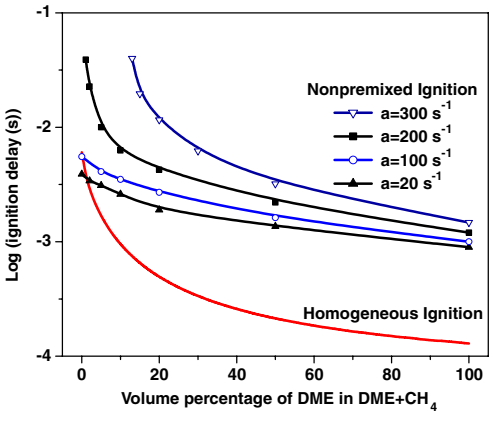

Fig. 3. Effects of DME addition on ignition delay of methane at atmospheric pressure (the initial temperature is 1400 K and $\phi = 1.0$ in the homogeneous ignition simulation; the temperature of fuel is 298 K and that of hot air is 1400 K in the non-premixed ignition simulation).

homogeneous ignition at initial temperature 1400 K show that the addition of DME to CH_4–air has a dramatic enhancement in CH_4–air ignition, particularly, at small amounts of DME addition. It is seen that for 10% of DME addition, the ignition time can be reduced by at least an order of magnitude. As the DME addition level reaches 40%, a further increase in DME blending has little effect on reducing ignition time. Furthermore, the ignition enhancement will also be a function of initial reaction temperature.

In order to understand the factors involved in the enhancement of methane ignition by DME addition, radical path, and computational singular perturbation (CSP) analyses [33] were made. Figure 4 shows the radical pool development (sum of CH_3, H, O, OH, HO_2, and C_2H_5) during ignition of DME/CH_4–air mixtures for various

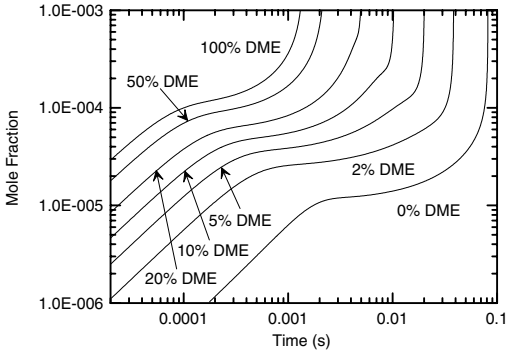

Fig. 4. Radical pool (H, O, OH, HO_2, CH_3, C_2H_5) growth during homogeneous ignition of DME/CH_4–air mixtures ($P = 1$ atm, $\phi = 1.0$, $T = 1200$ K).

levels of DME addition. Addition of a small amount of DME (i.e., 2%) drastically increases the radical pool concentration growth. As DME concentration further increases, however, this effect is lessened which gives rise to the nonlinear ignition enhancement observed in Fig. 3. CSP analyses were performed during the initial radical build-up stages to gain further insight into the reactions participating in this process (Fig. 5). The CSP methodology was implemented including temperature as one of the state variables [34], permitting thermokinetic feedback to be treated in the analyses. CSP has an advantage in comparison to typical sensitivity analysis methods in that the entire thermokinetically coupled system is treated directly and perturbation is applied to the complete set of differential equations describing the kinetic system.

For CH_4–air mixtures without DME the initial radical production is governed by the reaction $CH_4 + O_2 \rightarrow CH_3 + HO_2$, which has no significant contribution to radical pool growth later in the induction period. The methyl radicals formed react with O_2 to yield CH_2O and OH, or CH_3O and O, with CH_3O decomposing to form CH_2O and H. Through abstraction reactions, CH_2O forms HCO which subsequently yields HO_2 and CO through oxidation. The recombination reaction $2CH_3(+M) \rightarrow C_2H_6(+M)$ is the main channel opposing the initial radical pool growth. When both CH_3 and HO_2 are available in sufficient concentrations, $CH_3 + HO_2 \rightarrow CH_3O + OH$ becomes an important radical source. The above processes all depend on developing a significant pool of CH_3

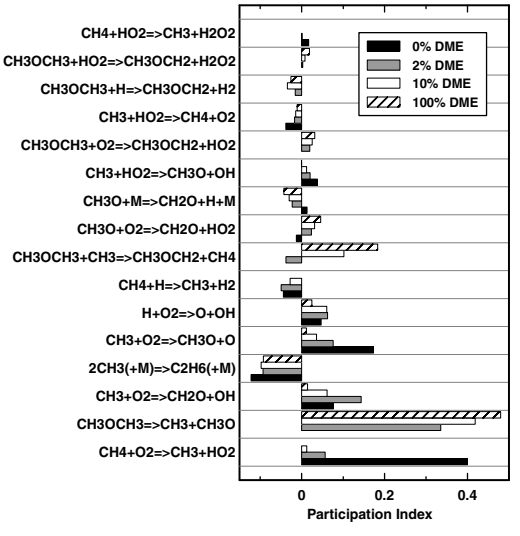

Fig. 5. Dominat reactions during initial radical build-up (DME/CH_4–air; $P = 1$ atm, $\phi = 1.0$, $T = 1200$ K) obtained from CSP analysis.

and HO_2 before radical pool growth of OH, O, and H can occur.

Since, the governing reaction $CH_4 + O_2 \rightarrow CH_3 + HO_2$ (Fig. 5) is slow relative to the similar reaction and/or thermal decomposition rates of higher alkanes, the ignition time for pure CH_4–air mixtures is, in comparison, relatively longer. Once a small amount of DME is present, the system is strongly driven by the unimolecular decomposition of DME (Fig. 5). This reaction is the major initial source of radicals and continues to contribute to radical production thereafter. With DME addition to methane, the radical pool growth occurs much more rapidly (Fig. 4), as it is not limited by the rate at which methyl radicals alone can produce more reactive species. In the case of DME, unimolecular decomposition yields CH_3O and CH_3 at the above temperatures, and subsequent abstraction reactions of CH_3 and radicals generated from CH_3O produce CH_3OCH_2 which in turn yields additional radical growth through decomposition to CH_3 and CH_2O. These reaction sequences lead to a relatively large concentration of HO_2, which in turn provides an alternative mechanism for CH_3 to yield radicals ($CH_3 + HO_2$ vs. $CH_3 + O_2$). CH_2O reacts with OH, H, or CH_3 through $CH_2O + X \rightarrow HCO + X$ ($X = OH$, O, H, and CH_3). Formyl radicals further oxidize to produce CO and HO_2. CH_3O decomposes through $CH_3O + M \rightarrow CH_2O + H + M$, or reacts with O_2 to obtain CH_2O and HO_2. Moreover, the large concentrations of HO_2 also produce H_2O_2 and subsequent production of OH through $H_2O_2 + M \rightarrow OH + OH + M$. Thus, by DME addition to methane not only is CH_3 more easily generated, other sources and channels are also available for generating radicals, as a result it enhances ignition.

The effect of DME addition on ignition time in non-premixed counterflow systems is also shown in Fig. 3. It is seen that, unlike the homogenous case, the ignition enhancement strongly depends on the stretch rate. At large stretch rates, the ignition is kinetically limited (the characteristic transport time is shorter than that of ignition) so that a small amount of DME addition causes a rapid reduction of ignition time. For example, at a high stretch rate ($a = 300\ s^{-1}$), the short flow residence time prevents the slow radical process from quickly building up the radical pool, so that the ignition time of pure methane in non-premixed counterflow is considerably long. It is a kinetic limited process. However, at low stretch rates, the ignition time is limited by the characteristic transport time (transport limited). In this regime, the ignition time only slightly decreases with increasing DME concentration. Furthermore, it is noted that for both low and high stretch rates, the minimum ignition times for large amounts of DME addition are of the same order, indicating the limiting by transport as the kinetic ignition time is shortened. Therefore, it can be concluded that for non-premixed ignition, there are two different regimes. In the kinetic limited regime, DME addition will significantly reduce the ignition time. However, in the transport limited regime, the ignition enhancement by DME addition is much less significant.

Besides, Fig. 3 shows that, for very low DME percentages, the homogeneous ignition time is larger than that of non-premixed ignition at low strain rates. This is caused by the presence of transport in nonpremixed ignition. For nonpremixed ignition, thermal, and mass transports have two effects: (1) to bring heat to the ignition kernel and preheat the fuel by the hot air, and (2) to move away the radicals produced in the ignition kernel, slowing down the radical pool growth. In cases of low strain rates of large ignition delay times, the first effect becomes important because the endothermic decomposition reactions of DME are enhanced by the convective heat transfer and the radical transported away from the ignition kernel is low at small radical gradients.

To further demonstrate the stretch and DME addition effects on methane ignition in non-premixed configuration, the evolution of the maximum mass fraction of CH_3, the major radical species controlling the ignition time, as discussed previously, is shown in Fig. 6. It is seen that with increasing DME addition (from 2% to 10%), similar to the homogeneous case, the ignition time is reduced, however, its effect greatly depends on the stretch rate. For example, at low stretch rate ($20\ s^{-1}$), the ignition is only slightly enhanced when the DME addition changes from 2% to 10%, although the initial CH_3 concentration is heavily affected. On the other hand, at high stretch rate ($200\ s^{-1}$), ignition time is significantly shortened by increasing the DME addition from 2% to 10%. This result further confirms the existence

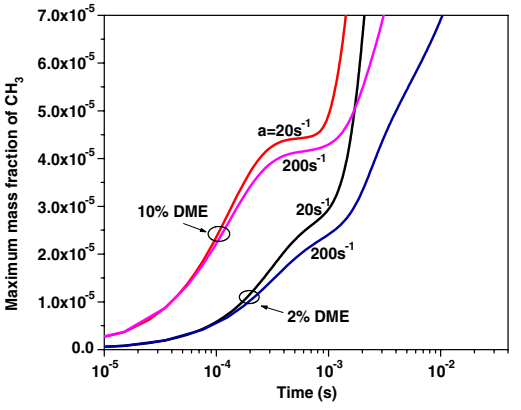

Fig. 6. Evolution of the maximum mass fraction of CH_3 in non-premixed ignition at different stretch rates and DME addition levels.

of two different regimes for non-premixed ignition.

3.2. Laminar flame speeds of DME/CH_4 binary fuel mixtures

Figure 7 shows the dependences of the measured and predicted laminar flame speeds of DME blended methane–air flames on the DME addition level at different equivalence ratios. It is seen that with the increasing amounts of DME, the laminar flame speeds of DME/CH_4–air flames increase almost linearly with the addition, although the rate of increase is slightly larger at small DME addition levels. In addition, the numerical results calculated from the 2006-mechanism agree reasonably well with the experimental data. This result indicates that although DME addition can increase the initial radical production for the acceleration of ignition, the fuel oxidation rate which is dominated by chain-propagation and termination reactions does not change significantly. As a result, the burning speed of a binary fuel mixture can be approximated as a linear function of the mixture fraction of the blended fuel.

3.3. Extraction of markstein length and global lewis number

Figure 8 shows the unburned Markstein lengths L_u of DME blended methane–air flames at different equivalence ratios and DME concentrations. The unburned Markstein length was obtained directly from the linear flame relation $S_u = S_u^0 - L_u K$, where K is the flame stretch [20]. It is seen that for pure methane–air flames ($\alpha = 0$), the unburned Markstein length increases with the equivalence ratio. The present data agree well with those measured by Rozenchan et al. [35]. It is well-known that the Lewis number of lean

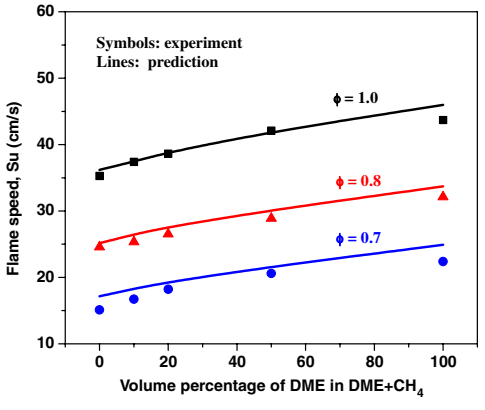

Fig. 7. Variation of laminar flame speeds of DME/CH_4–air mixtures at different equivalence ratios and DME blending at 298 K, atmospheric pressure.

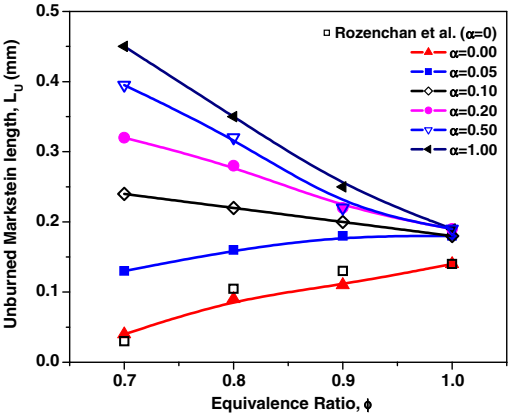

Fig. 8. Unburned Markstein lengths of DME/CH_4–air flames as a function of equivalence ratio at different amount of DME blending at 298 K, atmospheric pressure.

methane–air mixtures is slightly less than unity. This positive dependence on equivalence ratio is due to an increase in the effective Lewis number as the mixture approaches stoichiometric conditions [36]. When DME is added to CH_4, it is interesting to see that the unburned Markstein length increases significantly. In contrast to the linear dependence of flame speed on DME addition described above, the Markstein length increases more than 50% with only 10% DME addition. In addition, the Markstein length starts to have a negative dependence on the equivalence ratio for DME levels larger than 10%. This nonlinear dependence on DME addition to the binary fuel has not been reported in the literature.

The rapid increase of unburned Markstein length by small amounts of DME addition implies that the global Lewis number or the overall Zel'dovich number (β) of the mixture is very sensitive to DME addition. The Zel'dovich number can be computed from the sensitivity of flame speed to the adiabatic flame temperature. The global Lewis number of the mixture can be extracted from the measured unburned Markstein length according to the following relation [37]:

$$\frac{L_u}{\delta} = \frac{\sigma}{1-\sigma}\left[\frac{\beta(Le-1)}{2}\cdot\int_0^{(1-1/\sigma)}\frac{\ln(1+x)}{x}\mathrm{d}x - \ln(\sigma)\right], \quad (1)$$

where δ is the flame thickness, σ the ratio of burned and unburned gas densities, and β the Zel'dovich number.

Figure 9 shows the dependences of the global Lewis number, Zel'dovich number, and unburned Markstein length on the percentage of DME addition at $\phi = 0.8$. It is seen that the activation energy decreases quickly with the DME addition. This is because the DME addition promotes the radical

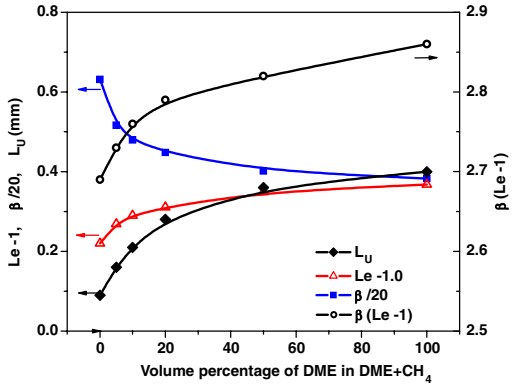

Fig. 9. Effects of DME addition on the global Lewis number, Zel'dovich number and unburned Markstein lengths of DME/CH_4–air flames at 298 K, atmospheric pressure, and $\phi = 0.8$.

pool growth shown in Fig. 4. However, it also causes rapid increase of the overall Lewis number. As a result, the reduced Lewis number, $\beta(Le - 1)$, increases significantly with a small addition of DME. Therefore the Markstein length nonlinearly depends on DME addition level.

4. Conclusions

In the present work, the effects of DME addition to methane–air mixtures on ignition, flame speeds, and Markstein length were studied experimentally and computationally. New experimental data were obtained for the study of kinetic coupling between DME and methane and for the validation of existing kinetic mechanisms. The following conclusions can be drawn from the present work:

1. In homogeneous ignition, small amounts of DME addition to methane lead to a significant decrease in ignition time. The effect is even more profound than that of hydrogen addition. This significant ignition enhancement is caused by the rapid build-up of CH_3 and HO_2 radicals when DME addition is present in the system. The resulting chain propagation reaction via CH_3 and HO_2 replaces the slow reactions via CH_3 and O_2 in the pure methane case and thus accelerates the ignition.
2. In non-homogeneous ignition, it is found that the ignition enhancement is strongly affected by the stretch rate. There exist two ignition regimes: a kinetic limited regime and a transport limited regime. In the kinetic limited regime, small amounts of DME addition cause a dramatic decrease of ignition time. However, in the transport limited regime, ignition enhancement by DME addition is much less effective.
3. In contrast to the nonlinear behavior in ignition enhancement, the flame speeds of DME/CH_4–air mixture are linearly proportional to the DME fraction. However, it is shown that small amount of DME addition leads to a significant change in Markstein length, effective Lewis number, and the overall activation energy.
4. The comparison between the experimental data with model predictions showed that the 2000-Mech, 2003-Mech, and 2005-Mech do not well reproduce the flame speed data for both DME and methane–air flames, although 2005-Mech performs much better than its previous versions. The results also showed that the recently developed mechanism (2006-Mech) is able to well reproduce the speeds of both DME–air and methane–air flames, and those for DME addition to methane.

Acknowledgments

The authors thank Professor H.J. Curran at the University of Ireland for providing his chemical mechanism. This work was partially supported by PRF#39162-AC9 and Air Force Research F49620-04-1-0038 and the Chemical Sciences, Geosciences and Biosciences Division, Office of Basic Energy Sciences, US Department of Energy under Grant No. DE-FG02-86ER13503.

Appendix A. Supplementary data

Supplementary data associated with this article can be found in the online version at doi:10.1016/j.proci.2006.07.177.

References

[1] T. Fleisch, C. McCarthy, A. Basum, C. Udovich, P. Charbonneau, W. Slodowske, S. Mikkelsen, J. McCandless, *SAE*-95-0061, 1995.
[2] U. Pfahl, K. Fieweger, G. Adomeit, *Proc. Combust. Inst.* 26 (1996) 781–789.
[3] B.L. Edgar, R.W. Dibble, D.W. Naegeli, *SAE*-97-1677 (1997).
[4] K. Wakai, K. Nishida, T. Yoshizaki, H. Hiroyasu, *The 4th Int. Symp. COMODIA 98*, Kyoto, Japan, 1998, p. 537.
[5] V.I. Golovitchev, N. Nordin, F. Tao, J. Chomiak, *CERC annual report*, CTH publication Nr. 99/2, Goteborg, 1999.
[6] T. Amano, F.L. Dryer, *Proc. Combust. Inst.* 27 (1998) 397–404.
[7] P. Dagaut, J.C. Boettner, M. Cathonnet, *Proc. Combust. Inst.* 26 (1996) 627–632.
[8] H.J. Curran, W.J. Pitz, C.K. Westbrook, P. Dagaut, J.-C. Boettner, M. Cathonnet, *Int. J. Chem. Kinet.* 30 (1998) 229–241.

[9] S.L. Fischer, F.L. Dryer, H.J. Curran, *Int. J. Chem. Kinet.* 32 (2000) 713–740.
[10] H.J. Curran, S. Fischer, F.L. Dryer, *Int. J. Chem. Kinet.* 32 (2000) 741–759.
[11] H.J. Curran, private communication, (2005).
[12] E.W. Kaiser, T.J. Wallington, M.D. Hurley, J. Platz, H.J. Curran, W.J. Pitz, C.K. Westbrook, *J. Phys. Chem. A* 104 (2000) 8194–8206.
[13] B. McIlroy, T.D. Hain, H.A. Michelsen, T.A. Cool, *Proc. Combust. Inst.* 28 (2000) 1647–1653.
[14] X.L. Zheng, T.F. Lu, C.K. Law, C.K. Westbrook, H.J. Curran, *Proc. Combust. Inst.* 30 (2005) 1101–1109.
[15] C.A. Daly, J.M. Simmie, J. Wurmel, N. Djebaili, C. Paillard, *Combust. Flame* 125 (2001) 1329–1340.
[16] Z. Zhao, A. Kazakov, F.L. Dryer, *Combust. Flame* 139 (2004) 52–60.
[17] X. Qin, Y. Ju, *Proc. Combust. Inst.* 30 (2005) 204–233.
[18] Y. Xue, Y. Ju, *Combust. Sci. Technol.* in press.
[19] M. Yao, J. Qin, *The Seventh Asia-Pacific International Symposium on Combustion and Energy Utilization*, Hong Kong, 2004, Paper 90-3.
[20] P. Clavin, *Prog. Energy Combust.* 11 (1985) 1–59.
[21] Z. Zhao, M. Chaos, A. Kazakov, F.L. Dryer, *Int. J. Chem. Kinet.* submitted.
[22] S. Kwon, L.K. Tseng, G.M. Faeth, *Combust. Flame* 90 (1992) 230–246.
[23] R.J. Kee, J.F. Grcar, M.D. Smooke, J.A. Miller, Report No. SAND85-8240, Sandia National Laboratories, 1985.
[24] A.E. Lutz, R.J. Kee, J.A. Miller, Report No. SAND87-98248, Sandia National Laboratories, 1987.
[25] Y. Ju, H. Guo, K. Maruta, F. Liu, *J. Fluid Mech.* 342 (1997) 315–334.
[26] Y. Ju, C.K. Law, K. Maruta, T. Niioka, *Proc. Combust. Inst.* 28 (2000) 1891–1900.
[27] Z. Zhao, *Experimental and Numerical Studies of Burning Velocities and Kinetic Modeling for Practical and Surrogate Fuels*, Ph.D. thesis, Princeton University, 2005.
[28] J. Li, Z. Zhao, A. Kazakov, F.L. Dryer, *Int. J. Chem. Kinet.* 36 (2004) 566–575.
[29] J. Li, *Experimental and Numerical Studies of Ethanol Chemical Kinetics*, Ph.D. thesis, Princeton University, 2004.
[30] J. Li, A. Kazakov, F.L. Dryer, *2nd European Combustion Workshop*, Louvain-la-Neuve, Belgium, 2005, Poster R15-019.
[31] J. Li, Z. Zhao, A. Kazakov, F.L. Dryer, *Int. J. Chem. Kinet.* submitted.
[32] P. Dagaut, C. Daly, J.M. Simmie, M. Cathonnet, *Proc. Combust. Inst.* 27 (1998) 361–369.
[33] S.H. Lam, *Combust. Sci. Technol.* 89 (1993) 375–404.
[34] A. Kazakov, M. Chaos, Z. Zhao, F.L. Dryer, *J. Phys. Chem A* 110 (2006) 7003–7009.
[35] G. Rozenchan, D.L. Zhu, C.K. Law, S.D. Tse, *Proc. Combust. Inst.* 29 (2002) 1461–1469.
[36] G. Joulin, T. Mitani, *Combust. Flame* 40 (1981) 235–246.
[37] P. Clavin, F.A. Williams, *J. Fluid Mech.* 116 (1982) 251–282.